# The Spider DMA: A miniature radial differential mobility analyzer

Stavros Amanatidis[1], Changhyuk Kim[1,3], Steven R. Spielman[2], Gregory S. Lewis[2], Susanne V. Hering[2], Richard C. Flagan[1,*]

[1] *Division of Chemistry and Chemical Engineering, California Institute of Technology, Pasadena, California, USA*

[2] *Aerosol Dynamics Inc., Berkeley, California, USA*

[3] *Department of Environmental Engineering, Pusan National University, Busan, Republic of Korea*

*Corresponding author: flagan@caltech.edu, 1200 E. California Blvd. M/S 210-41, Pasadena, CA 91125, USA, phone: +1 (626) 395 4383, fax: +1 (626) 568 8743

# *Supplementary Material*

Figure S1 shows a 3D simulation (bottom view) of the inlet sample flow distribution around a Spider DMA classifier entrance employing a tangential aerosol inlet. In this example, a 0.3 L/min inlet flow is introduced tangentially through a 4.5 mm inlet diameter tube into a 2-mm wide annulus (i.e., "racetrack") that distributes the flow around the classifier. Downstream the racetrack, a 0.8 mm "knife edge" gap provides an annular entrance for azimuthal distribution of the flow. At the design flowrates, the simulation reveals that the flow is distributed only about half-way around the classifier perimeter, leading to a highly non-uniform azimuthal distribution of flow velocities with a maximum near the point where the tangential inlet enters the racetrack. Because of this maldistribution of the flow, this tangential inlet approach would lead to significantly lower DMA resolution and transmission efficiency than the simplified design equations



ibution by providing a higher pressure drop as the flow enters the classification region, but at a cost of very tight manufacturing tolerances to maintain a uniform gap around the classifier.

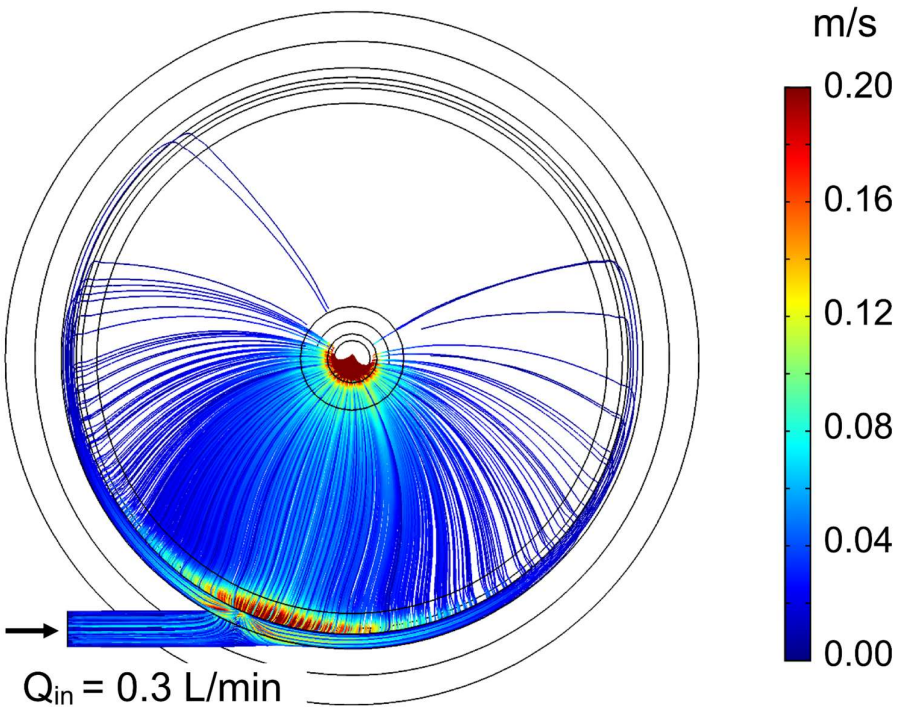


Figure S1 Simulated flow streamlines in the Spider DMA with a tangential entrance approach for 0.3 L/min sample inlet flow. A 2 mm "racetrack" with a 0.8 mm knife edge gap was considered as the flow distribution geometry.

Figure S2a shows the curved flow distribution channels in the Spider DMA inlet flow housing. The inlet sample is introduced into the port that is offset from the center, where the central port comprises the excess flow outlet. The incoming flow is distributed into the curved channels that provide the sample into a 1 mm-wide annulus. To further distribute the flow in the azimuth between the channels, an array of 0.5 mm holes are positioned at its outlet. The spacing of these holes, demonstrated in Figure S2b, has been tuned for uniform azimuthal distribution of the flow around the classifier entrance.

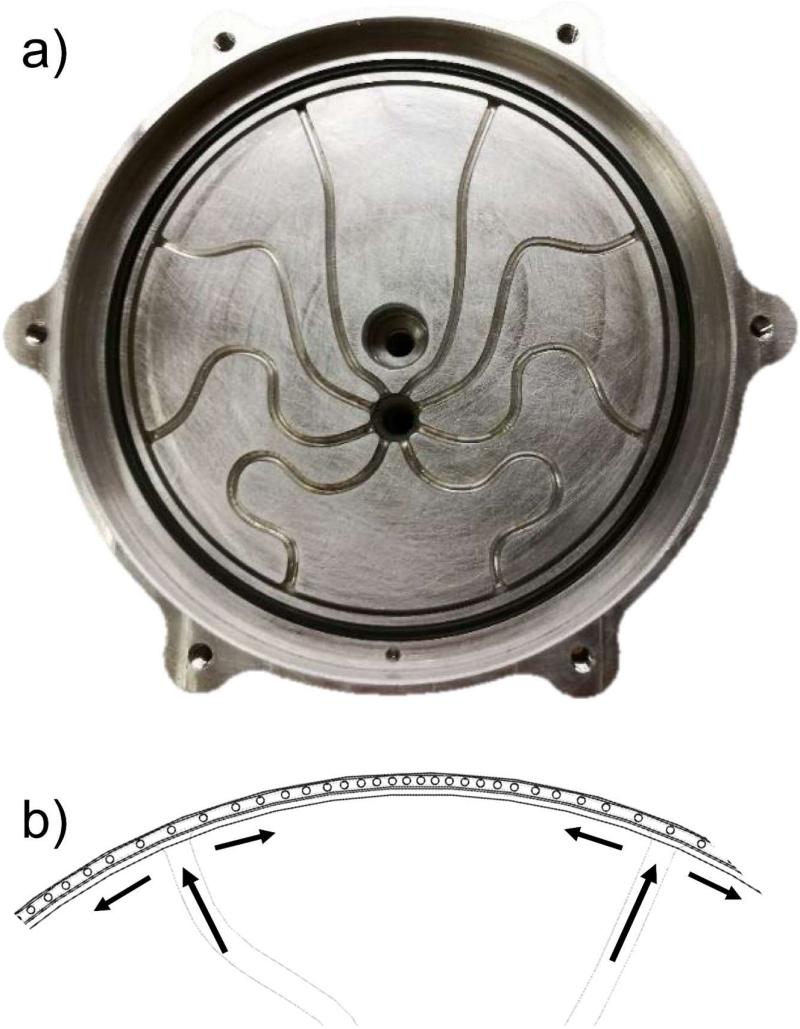


Figure S2 a) Top view of the prototype Spider DMA sample inlet housing, featuring the design of the "spider" flow distribution channels. b) Schematic of the Spider DMA classification region entrance, consisting of a 1 mm annular slot combined with an array of 0.5 mm holes at its outlet. Arrows indicate the effect of the holes on distributing the incoming flow in the azimuth between the curved flow channels.

Figure S3a compares the variation of the transfer function diffusional broadening parameters $\tilde{\sigma}^*$ (dashed line), $\tilde{\sigma}^*_{\mathrm{fit}}$ (symbols), and $\tilde{\sigma}^*_{\mathrm{eff}}$ (solid line) with $\mathrm{Pe}^*_{\mathrm{mig}}$; these correspond to Eqs. (9), (12), and (21) respectively, in the manuscript. At low $\mathrm{Pe}^*_{\mathrm{mig}}$, where $\tilde{\sigma}^*$ is high because of Brownian particle motion, $\tilde{\sigma}^*_{\mathrm{fit}}$ values agree well with the Stolzenburg model prediction. As $\mathrm{Pe}^*_{\mathrm{mig}}$ inscreases, the relative contribution of the distortion component, $\tilde{\sigma}_{\mathrm{d}}$, becomes more significant, resulting in deviating $\tilde{\sigma}^*$ and $\tilde{\sigma}^*_{\mathrm{fit}}$ curves. In the non-diffusive operating range ($\mathrm{Pe}^*_{\mathrm{mig}}$>10,000), $\tilde{\sigma}^*_{\mathrm{fit}}$ values asymptotically approach the value of $\tilde{\sigma}^*_{\mathrm{d}}$ as $\tilde{\sigma}^*$ approaches zero ($\tilde{\sigma}_{\mathrm{fit}}{}^2 = \tilde{\sigma}^2 + \tilde{\sigma}_{\mathrm{d}}^2$). Using a constant

additive distortion parameter yields a $\tilde{\sigma}^*_{\text{eff}}$ that agrees well with the $\tilde{\sigma}^*_{\text{fit}}$ values over the entire $\text{Pe}^*_{\text{mig}}$ range. The resolution of the mRDMA, shown in Figure S3b, asymptotically approaches 2.75 in the non-diffusive operating range, about 9% lower than that predicted by the flowrate ratio, i.e., $R_{\text{ND}} = \beta^{-1}$, owing to the non-ideal azimuthal flow distribution at the classifier entrance.

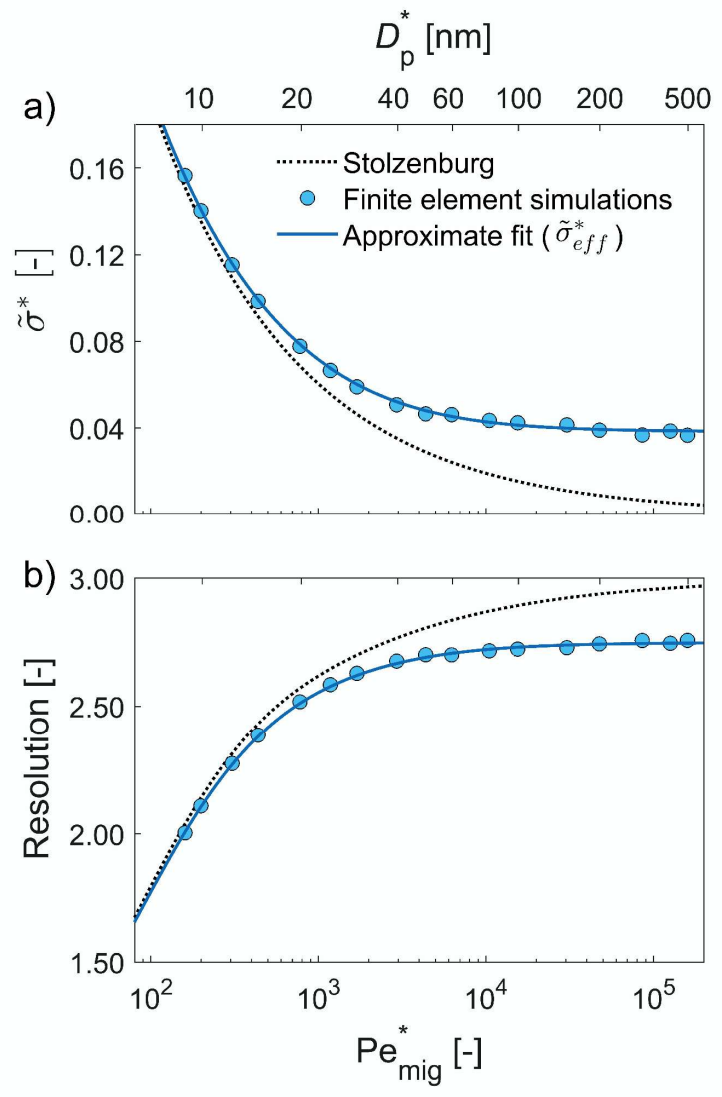


Figure S3 Comparison between the theoretical and simulated broadening of the transfer function width: a) Broadening parameter $\tilde{\sigma}^*$, and b) Spider DMA resolution, as a function of $\text{Pe}^*_{\text{mig}}$ (bottom axes) and corresponding particle size, $D^*_{\text{p}}$, (top axes) for 0.9/0.3 L/min Spider DMA sheath/sample flowrates.

Figure S4 shows the simulated Spider DMA transfer function assuming ideal azimuthal distribution of both sample and sheath flows around the classifier entrance, for 200 nm particles. The finite element simulations have been performed based on a Spider DMA geometry with a classifier entrance consisting of only the 1 mm annular slot (i.e., excluding the 0.5 mm holes), albeit with an ideally uniform azimuthal flow distribution. The resulting simulated transfer function, which was fit with the parameterized transfer function model described in Eq. (13) in the manuscript, is in close agreement to the triangular shape of the theoretical prediction. Non-uniform azimuthal flow distribution will result in lower resolution and transmission efficiency from this ideal.

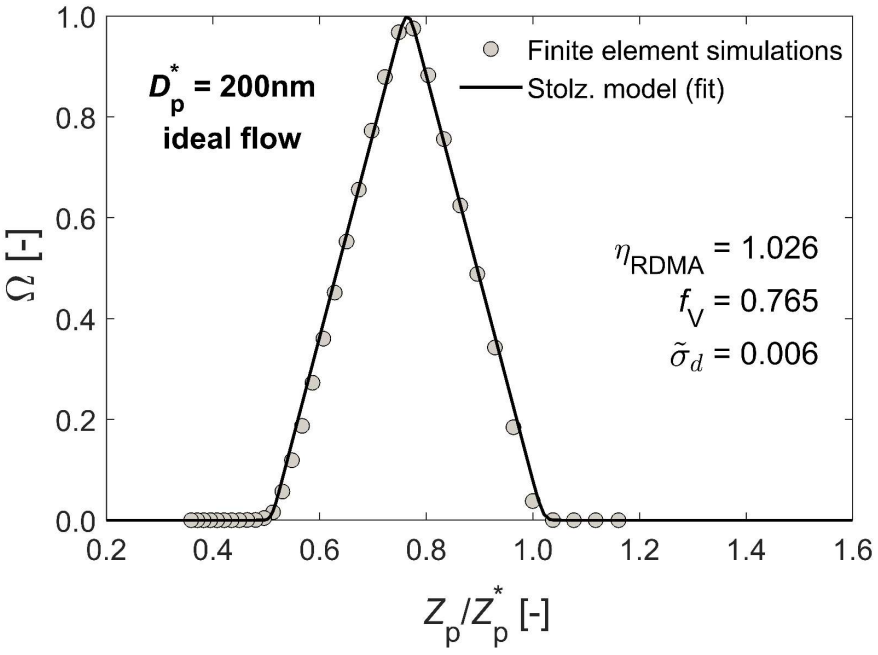


Figure S4 Simulated Spider DMA transfer function with ideal flow distribution in the classifier entrance, for $D_p^*$ = 200 nm and 0.3/0.9 L/min sample/sheath flowrates. Symbols show finite elements simulation data results. Solid lines demonstrate fits to the simulation data based on a parameterized model of the theoretical transfer function. $\eta_{RDMA}$, $f_V$, and $\sigma_{distor.}$ are the fitting parameters for transmission efficiency, mobility offset, and transfer function width, respectively.

Figure S5 compares the modeled Spider DMA response to experimental data using reference-size PSL particles. The response was measured in stepping-voltage mode with 152 ± 3 nm and 303 ± 6 nm PSL particles, for 0.75 – 1.20 L/min sheath flow and a 0.30 L/min sample flow, that correspond to a non-diffusive resolution in the $R_{ND}$ = 2.5 – 4.0 range. The Spider DMA predicted response, which is based on finite element simulations of the instrument transfer functions, is in close agreement with the experimental PSL data. Operating the instrument at different flowrate ratios, and corresponding values of $R_{ND}$, is

reflected in the shape of the transfer functions, which become more narrow as the sheath flow increases with constant sample flow. Moreover, increasing the sheath flow shifts the response peaks toward higher voltages, as these counterbalance the relatively shorter time available for charged particles to migrate across the gap between the classifier electrodes.

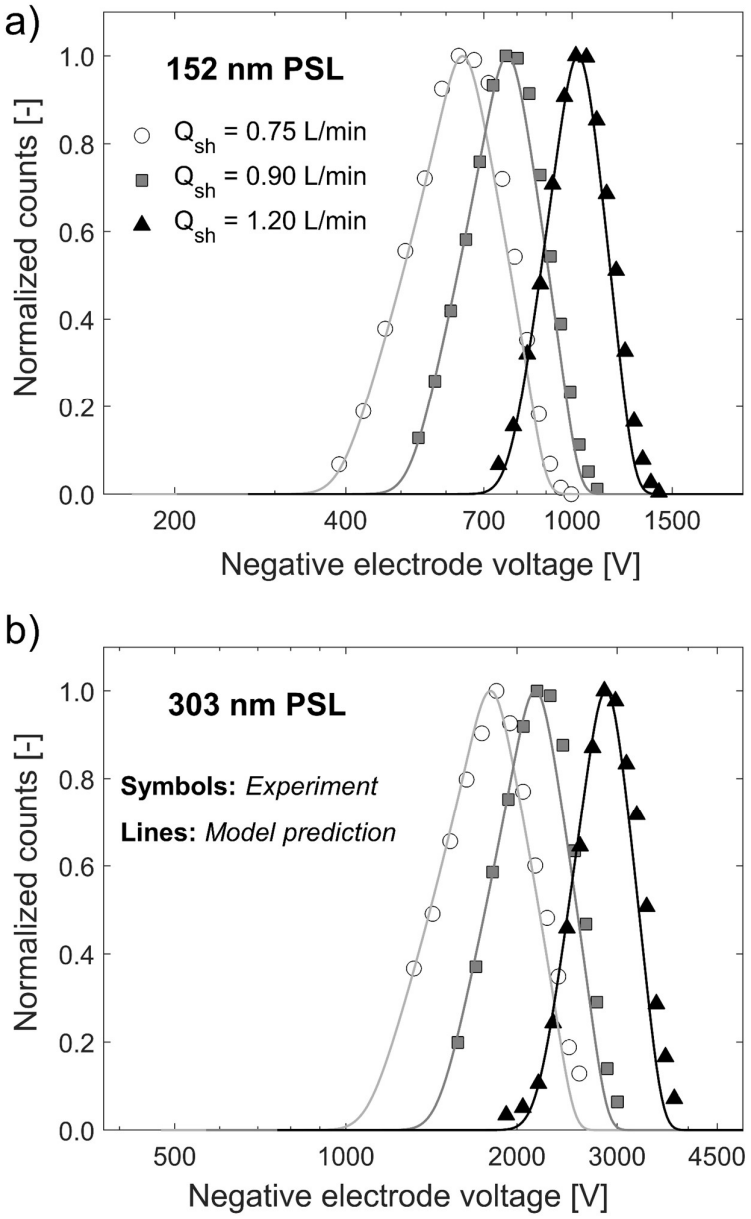


Figure S5 Normalized PSL particle counts versus applied electrode voltage for 0.75, 0.90, and 1.20 L/min sheath flowrates, and a 0.30 L/min sample flowrate, with a) 152 ± 3 nm PSL spheres, and b) 303 ± 6 nm PSL spheres. Counts are normalized with respect to peak measured values. Symbols show experimental data points; solid lines demonstrate model predicted response (scaled to 100% transmission efficiency).